Experimental Thermal and Fluid Science 49 (2013) 86–93

Contents lists available at SciVerse ScienceDirect

Experimental Thermal and Fluid Science

journal homepage: www.elsevier.com/locate/etfs

Displacement of liquid droplets on micro-grooved surfaces with air flow

Haibao Hu *, Suhe Huang, Libin Chen

College of Marine, Northwestern Polytechnical University, Xi'an 710072, China

ARTICLE INFO

Article history:
Received 25 January 2013
Received in revised form 4 April 2013
Accepted 4 April 2013
Available online 17 April 2013

Keywords:
Microgroove
Droplet
Shear flow
Dynamic contact angle
Force balance model

ABSTRACT

We investigate experimentally the dynamics of a liquid droplet that displaces on the micro-grooved surfaces driven by a controlled air flow. A range of experiments were carried out on the surfaces which patterned micro grooves with different directions and dimensions. The velocity required to initiate droplet motion increased with the grooves' dimensions. Displacement was obtained easier on the parallel micro-grooved surfaces compare to the vertical micro-grooved surface. Then a force balance model was constructed based on the capillary force and driving force. The analytical results were well consistent with the experiments. We suggest that the force model could be exploited in a reasonable estimate for the initiation velocity on a micro-grooved surface.

Published by Elsevier Inc.

1. Introduction

The formation and motion of droplets on surfaces exist widely in nature, traffic, new energy, fields of aviation and spaceflight and so on [1–3]. The motion of droplets can be induced by many different forces, for example electrostatic forces [4], the action of gravity [5], shearing forces exerted by the surrounding fluid [6,7], which has been the subject of intense study these decades. The study of droplet dynamics in a gas flow channel have been performed computationally [8]. Simulation works have also been carried out to investigate droplet deformation in a gas flow channel using the volume-of-fluid (VOF) method [9–11] and two-phase Lattice Boltzmann method (LBM) [12,13]. These research suggest that droplet motion with air flow is depends on the droplet size, properties of the liquids and surface topography.

Surface topography plays a dominant role during the droplet move on a solid surface by different forces. This can be understood from the following example. Consider a droplet move on a solid surface by the action of gravity, the footprint of the motion was not a straight line but a complex curve. Thanks to recent developments in micro-fabrication, it is possible to create a variety of surfaces with tailored wettability and physical morphology. Regular micro-grooved surface was one of these surfaces which have been used by many researchers to show that the drops impacting or rebounding process [14,15]. However, for the motion of droplets on a micro-grooved surface in a air flow have not been catch too much attention. In this paper, the initiation of liquid droplet motion on a micro-grooved surface, where the droplets are driven by a shearing airflow was considered experimentally. A simple analytical model, based on the forces acting on a moving droplet, is developed to predict droplet movement on a micro-grooved surface at the same time.

2. Materials and methods

2.1. Target surfaces

Finely polished copper plate surfaces of size 60 mm × 60 mm were used to prepare the target surfaces, using Quasi-LIGA molding technology. The target surfaces were signified by P_S^L and V_S^L with the superscript L designating the width of the micro-grooves and subscript S indicating the width of solid pillars between the different micro-grooves. The script P and V indicating parallel and vertical location of micro-grooved surfaces compare to the direction of air flow. In the present study, nine specimens were included according to different width of the micro-grooves and solid pillars. The pillars have different widths (0.2 mm, 0.3 mm and 0.4 mm) while the width of the micro-grooves changed (0.2 mm, 0.3 mm, 0.4 mm). However, the depths of the micro-grooves, D_G, were kept at 0.2 mm. Fig. 1 shows the representative microscope (HDM-600) images of the target surfaces. Contact angles against water which was shown in Table 1 were measured with a goniometer (OCA-20, Germany, 14 μL). The representative images of equilibrium contact angles on target surfaces were displayed in Fig. 3 which indicates a Wenzel state of wetting on the target surfaces. The advancing and receding angles were measured at the same time. It does indeed indicate that wetting behavior of droplets

* Corresponding author.
E-mail address: huhaibao@nwpu.edu.cn (H. Hu).

0894-1777/$ - see front matter Published by Elsevier Inc.
http://dx.doi.org/10.1016/j.expthermflusci.2013.04.005

Nomenclature

P	parallel location of micro-grooved surfaces
V	vertical location of micro-grooved surfaces
L–S	width of the micro-grooves and width of solid pillars (mm-mm)
R	radius of droplet (mm)
R_0	radius of truncated sphere (mm)
F	force exert on droplet (N)
U	velocity of air flow (m/s)
K	wall correction factor
H	height of the droplet (mm)
n	ratio between two axes
D_G	groove depth (mm)
Greek symbols	
ρ	droplet density (kg m^3)
σ	surface tension (N m^{-1})
μ	air viscosity (kg m^{-1} s^{-1})
θ	apparent contact angle (°)
γ	shear rate (s^{-1})
α	angular position (°)
Subscripts	
S	width of solid pillars (mm)
D	driving
C	capillary
X, Y	coordinate directions
con	constant
adv	advancing
rec	receding
Superscripts	
L	width of the micro-grooves (mm)

could be affected by micro grooves on the target surfaces. Detail relation between wetting behavior and dimensions of micro-grooves could be found in the experimental study Rahman et al. [16,17], which was not pursued here. A smooth surface was prepared to describe the role played by surface grooves on drop displacing process. Ultrasonic cleaner was used to clean the target surfaces before the start of each experiment.

2.2. Experimental method

The apparatus used in this experiment is shown schematically in Fig. 2. A wind tunnel of cross-section 110 mm × 60 mm and length 300 mm was used to measure the critical velocity required

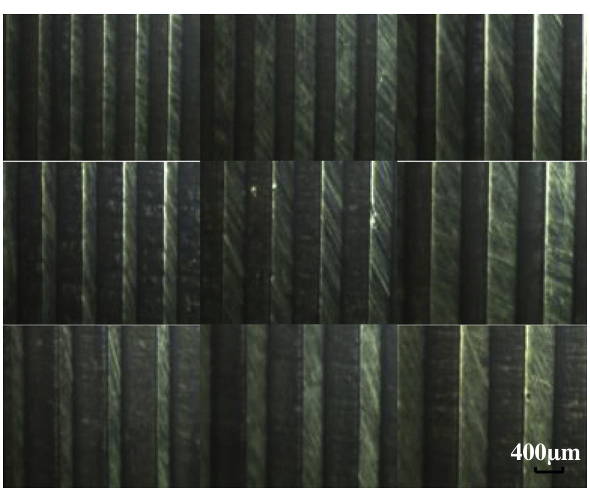

Fig. 1. Images of the target surfaces in a microscope.

to cause water droplet motion. Photographic techniques were employed to capture the physical events occurring during drop displace process. A CCD camera (IDT N4) was positioned above the wind tunnel to capture the entire event of droplet motion at 20 frames per second, with illumination provided by a 100 W halogen light source. However, the side section of the droplet was taken at the same time with another camera. The target surface was fixed at the bottom of a polymer wind tunnel in which a potentiometer was equiped to control the speed of the air flow. The bottom of the wind tunnel is removable so the target surfaces can be changed conveniently. Hot wire anemometer (TSI IFA300E) was used here to measure the velocity of the air flow which associated with voltage on the fan. Liquid droplets were generated by using a syringe pump so the volume of the droplet can be controlled accurately. For the droplet, distilled water with density, ρ = 996 kg/m^3, surface tension, σ = 0.073 N/m, and viscosity, μ = 0.001 kg/ms was used in the experiment.

At first, a liquid droplet generated on the tip of the syringe needle and gently lowered onto the surface. Subsequently, the fan was started and the velocity of the air was gradually increased until the droplet motion was initiated. Two CCD cameras were turned on to recording the process of displacement at the same time. Recording of the droplet displacement lasted less about 45 s and was stopped after the droplet moved out of the field of view. The pictures of experiment were treated by Image-ProPlus, the motion of droplet can be got by contrasting two successive pictures of experiment which will be detail explained next section. Then the critical velocity could be calculated from number of picture and gradient of voltage. The previous steps were repeated three times for each set of conditions and an average velocity was obtained. Droplet loss due to evaporation was proved to be minimal in this situation [18]. Typical uncertainty in the measured contact angle was

Table 1
Measurements of equilibrium and dynamic contact angles on different surfaces,

Surface sign	$V^{0.2}_{0.2}$	$V^{0.2}_{0.3}$	$V^{0.2}_{0.4}$	$V^{0.3}_{0.2}$	$V^{0.3}_{0.3}$	$V^{0.3}_{0.4}$	$V^{0.4}_{0.2}$	$V^{0.4}_{0.3}$	$V^{0.4}_{0.4}$
Contact angle (°)	110.71	96.32	89.99	93.88	100.87	90.66	88.28	87.56	80
Advancing angle (°)	115.63	107.7	102.33	114.89	109.48	102.75	110.11	103.26	99.97
Receding angle (°)	74.08	73.12	73.03	75.7	79.06	66.21	60.33	70.78	70.14
Surface sign	$P^{0.2}_{0.2}$	$P^{0.2}_{0.3}$	$P^{0.2}_{0.4}$	$P^{0.3}_{0.2}$	$P^{0.3}_{0.3}$	$P^{0.3}_{0.4}$	$P^{0.4}_{0.2}$	$P^{0.4}_{0.3}$	$P^{0.4}_{0.4}$
Contact angle (°)	75.43	78.72	69.97	71.96	67.61	63.97	66.37	71.47	60.12
Advancing angle (°)	100.09	97.99	94.56	96.59	91.52	86.37	83.9	93.45	84.44
Receding angle (°)	55.81	60.55	62.12	55.85	54.25	50.5	51	56.74	47.68

Download English Version:

https://daneshyari.com/en/article/651639

Download Persian Version:

https://daneshyari.com/article/651639

Daneshyari.com